Cell Tissue Res (2005) 319: 491–500
DOI 10.1007/s00441-004-1028-x

REGULAR ARTICLE

Karl Schumacher · Jürgen Klar · Charlotte Wagner · Will W. Minuth

Temporal-spatial co-localisation of tissue transglutaminase (Tgase2) and matrix metalloproteinase-9 (MMP-9) with SBA-positive micro-fibres in the embryonic kidney cortex

Received: 5 May 2004 / Accepted: 20 October 2004 / Published online: 25 January 2005

Abstract Growth of the kidney is a complex process piloted by the collecting duct (CD) ampullae. The dichotomous arborisation and consecutive elongation of this tubular element determines the exact site and time for the induction of nephrons in the overlaying mesenchymal cap condensates. The mechanism by which the CD ampullae find the correct orientation is currently unknown. Recently, we have demonstrated micro-fibres that originate from the basal aspect of the CD ampullae and extend through the mesenchyme to the organ capsule. The micro-fibres are assumed to be involved in the growth and arborisation process of the CD ampulla. Therefore, we have investigated the specific distribution of the micro-fibres during branching morphogenesis. We have also analysed whether the micro-fibres co-localise with extracellular matrix (ECM)-modulating enzymes and whether the co-localisation pattern changes during CD ampulla arborisation. Micro-fibres were detected in all stages of CD ampulla arborisation. Tissue transglutaminase (Tgase2) co-localised with soybean agglutinin (SBA)-positive micro-fibres, whose presence depended upon the degree of CD branching. Matrix metalloproteinase-9 (MMP-9) also co-localised with micro-fibres, but its expression pattern was different from that for Tgase2. Western blotting experiments demonstrated that Tgase2 and MMP-9 co-migrated with SBA-labelled proteins. Thus, the micro-fibres are developmentally modulated by enzymes of the ECM in embryonic kidney cortex. These findings illustrate the importance of micro-fibres in directing CD ampulla growth.

Keywords Stem cells · Kidney · Collecting duct · Development · Soybean agglutinin (SBA) · Tissue transglutaminase (Tgase2) · Matrix metalloproteinase-9 (MMP-9) · Rabbit (New Zealand)

K. Schumacher (✉)
Institute of Bioengineering and Nanotechnology,
A*STAR, # 04-01, 31 Biopolis Way,
The Nanos, 138669, Singapore
e-mail: kmschumacher@ibn.a-star.edu.sg

W. W. Minuth
Department of Molecular and Cellular Anatomy,
University of Regensburg,
93053 Regensburg, Germany

J. Klar · C. Wagner
Department of Physiology, University of Regensburg,
93053 Regensburg, Germany

Introduction

The metanephros anlage starts to develop from two markedly different embryonic tissues (Saxen 1987; Barasch et al. 1999; Dekel and Reisner 2004), namely the epithelial stem cells of the ureteric bud and the mesenchymal nephrogenic stem cells. Reciprocal interaction of both these tissues causes, on the one hand, the branching morphogenesis of the ureteric bud and, on the other hand, nephron induction in the mesenchyme. The first branching events of the ureteric bud determine the kidney poles and the three-dimensional structure of the later renal pelvis. Subsequent development involves the initiation of nephrogenesis. The ureteric bud is replaced by numerous CD ampullae found in precisely oriented vertical rows underneath the organ capsule. Ampulla nephrogenic mesenchymal cells within the cap condensate are located around the tip of each CD (Bard et al. 2001; Sariola 2002). The inductive action of a CD ampulla leads to an aggregation of a few mesenchymal cells forming the pretubular aggregate at the lateral side of the cap condensate. The CD ampulla then elongates and divides dichotomously again. Both the continuous process of longitudinal extension and the dichotomous branching of each CD ampulla determine the later histoarchitecture of the organ parenchyme. Thus, new generations of nephrons are continuously induced at defined sites depending on the growth direction of each of the CD ampullae. The volume of the organ increases by this mechanism continuously from the inner towards the outer cortex.

For the establishment of correct organ architecture, each of the CD ampullae must grow in an entirely linear direction

towards the organ capsule. This results in the establishment of absolutely straight collecting ducts. Whether the growth direction of each CD ampulla occurs randomly or whether the tissue follows a growth cue is unknown. Recently, we have detected soybean agglutinin (SBA)-positive micro-fibres lining the basal aspect of each CD ampulla through the mesenchyme and ending in the organ capsule (Schumacher et al. 2002a). These micro-fibres are found in the developing kidneys of human, mouse and rabbit. The specific localisation of the micro-fibres leads to the assumption that they structurally connect each of the CD ampullae, the mesenchyme and the organ capsule (Schumacher et al. 2002a; Schumacher et al. 2003). This structure could possibly explain the collecting tubule being constantly able to maintain an absolutely straight growth direction towards the organ capsule over extended periods of time during multiple steps of dichotomous branching.

In the present study, we investigate, for the first time, the arrangement of SBA-positive micro-fibres during branching of the CD ampulla by using morphological and cell-biological methods. We demonstrate that the micro-fibres persist in all stages of the branching process. In addition, we analyse the occurrence of oppositely acting tissue transglutaminase (Tgase2) and matrix metalloproteinase-9 (MMP-9) in relation to SBA-positive micro-fibres during the CD ampulla branching process. We demonstrate that the branching process does not occur randomly but is related to the structure of the extracellular matrix (ECM) consisting of SBA-positive micro-fibres.

Materials and methods

Tissue preparation

One-day-old New Zealand rabbits were anaesthetised with ether and killed by cervical dislocation. Both kidneys were removed immediately and then cut precisely along the cortico-medullary axis, frozen in liquid nitrogen and stored at −80°C until analysis.

Lectin incubation

Exactly oriented cortico-medullary cryosections (8 μm) of neonatal rabbit kidney were prepared by using a cryomicrotome (Microm, Heidelberg, Germany). The sections were fixed in ice-cold ethanol and then washed with phosphate-buffered saline (PBS). After incubation in blocking solution (PBS+1% bovine serum albumine+10% horse serum) for 30 min, the sections were exposed to fluorescein-isothiocyanate (FITC) conjugated soybean agglutinin (SBA; Vector Laboratories, Burlingame, USA) diluted 1:4,000 in blocking solution for 45 min. Negative controls were conducted by addition only of the secondary antibody. Following several washes in PBS the specimens were embedded with Slow Fade Light Antifade Kit (Molecular Probes, Eugene, USA) and analyzed using an Axioskop 2 plus microscope (Zeiss, Oberkochen, Germany). Images were taken with a digital camera and thereafter processed with Photoshop 5.5 (Adobe Systems, San Jose, CA, USA).

Co-incubation experiments with antibodies

Fluorescein-isothiocyanate (FITC)-conjugated SBA (Vector Laboratories, Burlingame, USA) was co-incubated with the following antibodies: anti-MMP-9 (Santa Cruz Biotechnology, Santa Cruz, USA), cytokeratin Endo A mab TROMA1, which was developed by Dr. P. Brulet and R. Kemler (University of Iowa, Department of Biological Sciences, Iowa City, IA 52242, under contract NO1-HD-7-3263 from the NICHD), and anti-tissue Tgase2 antibody, which was obtained from Neomarkers, Fremont, USA.

Before antibody incubation, 8-μm-thick cryosections of 1-day-old rabbit kidneys were fixed in ice-cold ethanol. After being washed in PBS, the sections were blocked with PBS containing 1% bovine serum albumin (BSA) and 10% horse serum for 30 min. Primary antibodies were applied for 1 h in blocking solution. The specimens were incubated for 45 min with donkey-anti-mouse- or donkey-anti-goat-IgG-Texas-red-conjugated secondary antibodies diluted 1:200 in PBS containing 1% BSA (Jackson Immunoresearch Laboratories, West Grove, USA) together with fluorescein-isothiocyanate (FITC)-conjugated SBA (Vector Laboratories) diluted 1:4,000. The sections were then analysed by using an Axioskop 2 plus microscope (Zeiss, Oberkochen, Germany). Images were taken with a digital camera and subsequently processed with Photoshop 5.5 (Adobe Systems, San Jose, Calif., USA).

Two-dimensional electrophoresis

Cortical explants of 1-day-old rabbit kidneys were isolated according to methods described earlier (Minuth 1987). Tissue samples were homogenised in lysis buffer (pH 7.5) containing 8 M urea, 4% CHAPS, 40 mM TRIS-HCL, 2 mM dithiothreitole and 0.5% carrier ampholytes. Aliquots of 300 μg protein sample were loaded onto a gel tube for isoelectric focusing. The gel tubes were run for 14 h at increasing voltage (100–1,000 V) in a model 175 Tube cell (Bio-Rad Laboratories, Hercules, USA). The focused gel tubes were equilibrated in a buffer containing 2% SDS, 10% glycerin, 125 mM TRIS-HCL and 1 mM EDTA and thereafter laid on the surface of 3-mm-thick 10% Laemmli gels in order to separate proteins by SDS-polyacrylamide gel electrophoresis (SDS-PAGE) at 100 V and 120 mA for 7 h. The gel plates were then stained with Serva blue R (SERVA, Heidelberg, Germany).

Western blotting with subsequent SBA, tissue Tgase2 and MMP-9 probing

In order to detect SBA-labelled molecules, two-dimensionally-separated proteins were electrophoretically transferred to polyvinylidene fluoride transfer membranes (Millipore, Bedford, USA). After exposure to PBS containing 10% horse serum and 0.02% Tween for 1 h, the membrane was incubated with SBA diluted 1:2,000 overnight at 4°C. After several washing steps, the membrane was incubated with antibody to SBA diluted 1:1,000 in PBS-Tween (anti-SBA; Vector Laboratories) followed by incubation with a horseradish-peroxidase-conjugated donkey anti-goat immunoglobulin antiserum (Dianova, Hamburg, Germany). Membranes were exposed to PBS containing 10% horse serum and 0.02% Tween for 1 h and then were incubated, for 2 h, with an anti-tissue Tgase2 antibody (Neomarkers, Fremont, USA) diluted 1:750 in PBS-Tween or with an anti-MMP-9 antibody (Santa Cruz Biotechnology) diluted 1:500 in PBS-Tween, followed by incubation with a horseradish-peroxidase-conjugated donkey anti-mouse immunoglobulin antiserum or with a horseradish-peroxidase-conjugated donkey anti-goat immunoglobulin antiserum (Dianova) diluted 1:1,500 in PBS-Tween for 45 min. Blot development was started by addition of 0.5 mg/ml diaminobenzidine, 0.02% H_2O_2 and 0.03% cobalt chloride dissolved in citrate buffer (17 mM, pH 6.3). The reaction was stopped by washing the membrane in tap water. Negative controls were conducted by the addition only of the secondary antibody. Immunoblots were documented with a Scan Jet 6,200 C scanner (Hewlett Packard, Greely, USA). Assessment of apparent molecular weight and isoelectric points was performed with two-dimensional SDS-PAGE standards, which were run in parallel experiments (Bio-Rad Laboratories, Hercules, USA).

Tissue isolation, detection of tissue Tgase2 mRNA by reverse transcription followed by polymerase chain reaction

The embryonic area of 1-day-old rabbit kidneys was isolated as described earlier (Minuth 1987). The mesenchymal cells and the capsula fibrosa were mechanically micro-

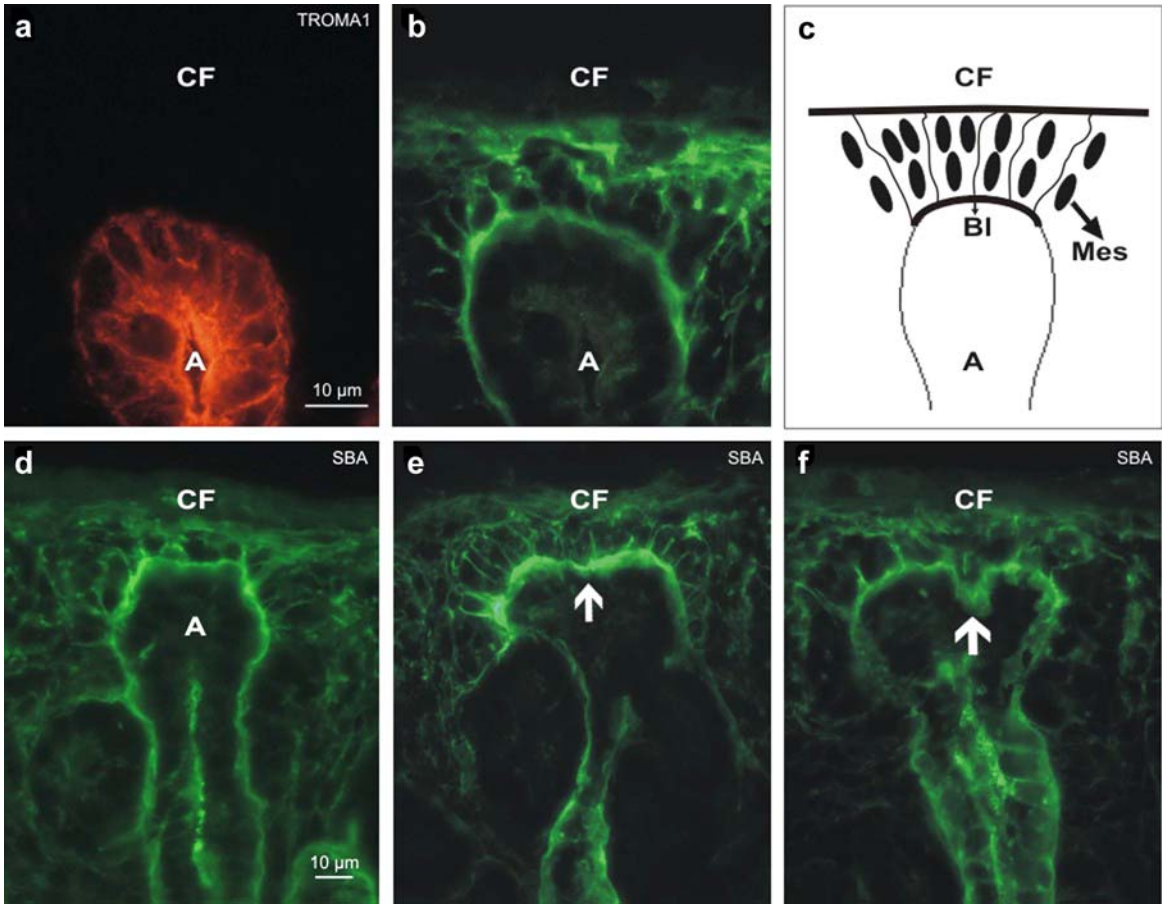

Fig. 1 SBA-positive fibres between the CD ampulla and capsula fibrosa (**a–c**). **a** Only CD ampulla epithelial cells are positive for TROMA1 (*CF* capsula fibrosa). **b** SBA-positive fibres are found between CD ampulla (*A*), mesenchyme and capsula fibrosa (*CF*). **c** SBA-positive fibres illustrated in a schematic representation (*A* CD ampulla, *CF* capsula fibrosa, *Bl* basal lamina, *Mes* mesenchymal cells). Occurrence of SBA-positive fibres during various developmental stages of CD ampulla branching (**d–f**). **d** Expression of SBA-positive fibres in non-branched CD ampulla. **e** Initiation of branching. A shallow cleft is visible (*arrow*). **f** A deep cleft between the arising buds is formed (*arrow*) in further branched stages. SBA-positive fibres are expressed in all three stages.

dissected from cortical explants under optical control of a KL 1500 stereo-microscope (Leica, Solms, Germany). The isolated tissue was collected in separate cups. To analyse the expression of Tgase2 mRNA or MMP-9 mRNA by reverse transcription followed by the polymerase chain reaction (RT-PCR), 2 μg total RNA of the various renal tissue preparations was reverse-transcribed by using standard protocols a in total volume of 20 μl. PCRs were

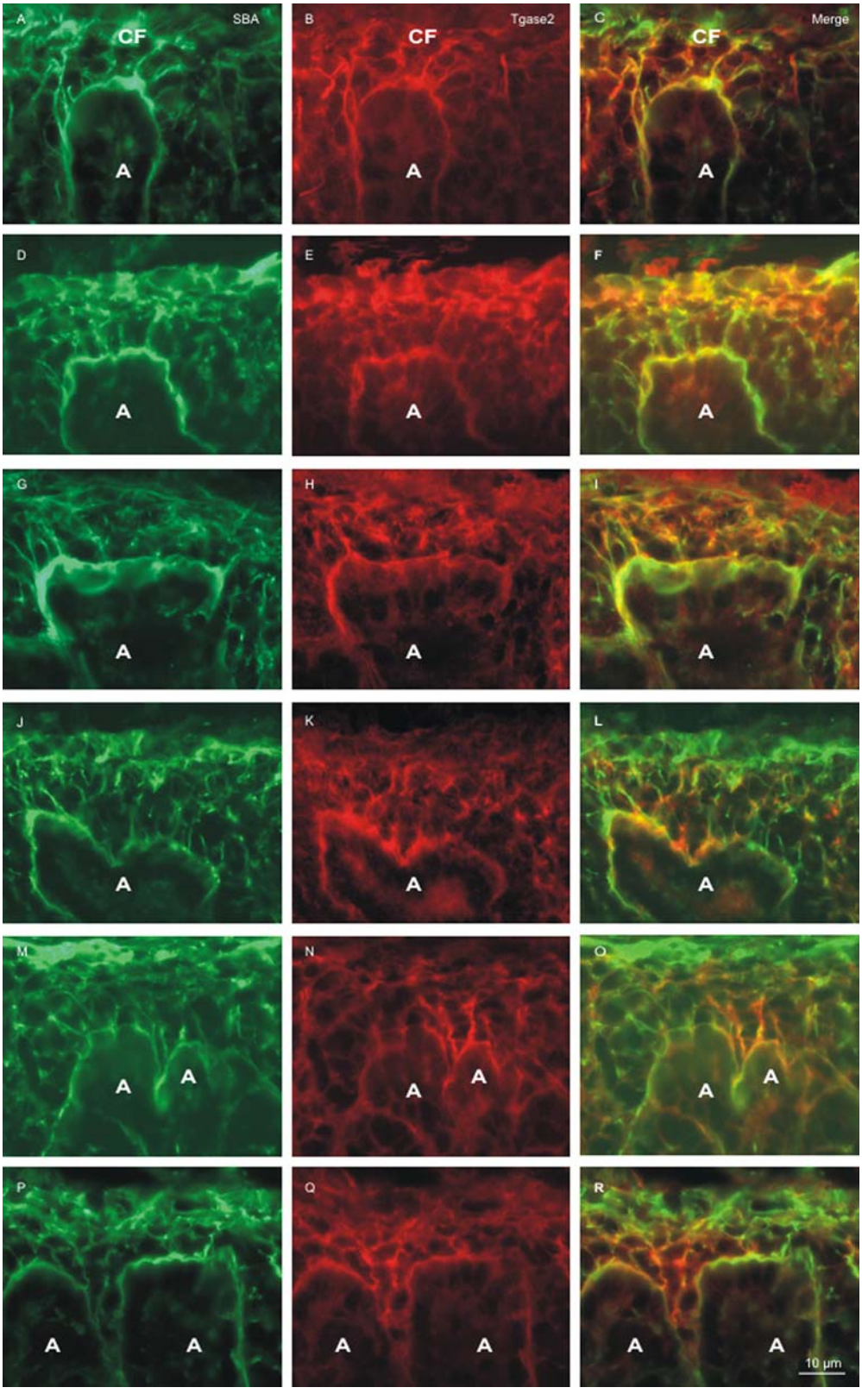

Fig. 2 Co-localisation of SBA-positive micro-fibres with the cross-linking ECM-enzyme Tgase2 at various developmental stages of CD ampulla branching (*A* CD ampulla, *CF* capsula fibrosa). *Left* SBA-label (**a, d, g, j, m, p**). *Middle* Label of Tgase2 (**b, e, h, k, n, q**). *Right* Merge image of the SBA label and the Tgase2 label (**c, f, i, l, o, r**). In non-branched CD ampulla (**a–f**) some micro-fibres display Tgase2 coexpression, but not all. Similar results are obtained from CD ampulla revealing initiation of branching (**g–i**). Investigation of stages with deep cleft formation (**j–r**) shows that the fibres near the cleft region; the related basal aspect of CD ampulla are intensively labelled for Tgase2.

performed in a total volume of 20 μl in the presence of 2 μl cDNA by using standard PCR protocols. Negative controls included water instead of cDNA in the PCR. Primers for Tgase2 (Kim et al. 2002) used for amplification of the 302-bp fragment were as follows: 5′ gcgcttccggctgacactgtact 3′ (forward) and 5′ agcaggatgaagtgacccagcatg 3′ (reverse). Primers for MMP-9 (Kim et al. 2002; Tezuka et al. 1994) used for amplification of the 142-bp fragment were as follows: 5′ cagctggcagaggagtacctg 3′ (forward) and 5′ gtggcattatccagctcccc 3′ (reverse). For β-actin, we used 5′ gcgcgccactgtcgagtc 3′ (forward) and 5′ attgatggagaggtatat 3′ (reverse).

Thirty-six cycles were performed for the amplification of Tgase-2 and MMP-9 according to the following protocol: denaturation at 90°C for 60 s, annealing at 60°C for 60 s and extension at 72°C for 30 s. β-Actin was used as a standard.

Results

Peculiarities of the embryonic renal cortex

The induction of nephrons with subsequent volume expansion during kidney growth is controlled by the secretion of soluble factors between the CD ampulla and the surrounding cap condensate (Vainio et al. 1989; Plisov et al. 2001). This process occurs in waves and is piloted by the elongation and subsequent dichotomous branching of the CD ampullae. Labelling the embryonic cortex of neonatal rabbit kidney for TROMA1 reveals that the tip of each CD ampulla is not in direct contact with the organ capsule during branching but is constantly found at a distance of approximately 20 μm (Fig. 1a). Histochemical labelling with SBA further reveals an intensive reaction at the basal aspect of each CD ampulla (Fig. 1b). In addition, SBA-labelled micro-fibres arise from the basal aspect of each CD ampulla andd line the cap condensate and end in the organ capsule (Fig. 1b, c). Thus, the micro-fibres have a length of up to 20 mm. In the cap condensate, they are found between the mesenchymal cells. As shown previously, the micro-fibres originate from a unique fibre-network surrounding the basal aspect of each CD ampulla (Fig. 1c; Strehl and Minuth 2001a, b).

SBA-positive micro-fibres during branching morphogenesis

Whether the SBA-positive fibres are solitary elements or whether they are involved in the branching process of the CD ampulla remains unknown. Therefore, we have analysed both non-branched (Fig. 1b, d) CD ampullae and CD ampullae in different stages of branching (Fig. 1e, f). Non-branched CD ampullae and arising buds are associated with an average of 10 SBA-labelled micro-fibres. Independent of the stage of branching, the SBA-positive micro-fibres constantly form a corona emanating from the basal aspect of each CD ampulla and lines the cap condensate towards the organ capsule (Fig. 1d–f). In addition, the micro-fibres are visible during the formation of shallow (Fig. 1e) and of deep (Fig. 1f) clefts of the arising buds of branching CD ampullae.

Co-localisation of SBA-positive micro-fibres with Tgase2

Immunohistochemistry earlier demonstrated that the SBA-positive micro-fibres were not identical with known structural ECM proteins (Schumacher et al. 2003). Consequently, we were interested in identifying functional proteins in the ECM, proteins that may cooperate with SBA-positive micro-fibres during branching events. Tgase2 is known to stabilise components of the ECM. By using double-labelling histochemistry, we therefore determined the presence of this enzyme in the outer cortex of embryonic kidney (Fig. 2b, e, h, k, n, q) and analysed whether Tgase2 co-localises with SBA-positive micro-fibres (Fig. 2c, f, i, l, o, r). Tgase2 label is found at the basal aspect of CD ampullae and on micro-fibres in the mesenchyme (Fig. 2b, e, h, k, n, q). Merge images of label for SBA and Tgase2 displays that, in 96 analysed CD ampullae, an average of 25%–30% of all SBA-labelled micro-fibres are completely positive for Tgase2 (Fig. 2c, f, i, l, o, r). Vice-versa, Tgase2-label co-localises with SBA-labelled micro-fibres at 80%–90% (Fig. 2c, f, i, l, o, r) independent of the stage of CD ampulla branching. Some of the non-branched CD ampullae show SBA-positive micro-fibres that exhibit simultaneous label for Tgase2 (Fig. 2b, c), whereas others demonstrate a complete lack of co-localisation (Fig. 2e, f). Furthermore, we have found that the micro-fibres and the basal aspect of CD ampullae are strongly positive for Tgase2 in the region of cleft formation between arising CD ampulla buds. Most interestingly, surrounding mesenchyme at the lateral sites of dichotomously dividing CD ampullae exhibits a much weaker or even absent label for Tgase2 (Fig. 2m–r).

Co-localisation of SBA-positive micro-fibres with MMP-9

Unlike Tgase2, MMP-9 is known to be an ECM-degrading enzyme occurring in the metanephric mesenchyme during kidney development (Tanney et al. 1998). Therefore, we have analysed the expression of MMP-9 in co-localisation with SBA-positive micro-fibres. Double-labelling of SBA (Fig. 3a, d, g, j, m, p) and MMP-9 (Fig. 3b, e, h, k, n, q) reveals a partial co-localisation (Fig. 3c, f, i, l, o, r) but different from that found for the Tgase2 label (Fig. 2). In contrast to Tgase2, MMP-9 is found as a faint discontinuous dotted pattern at the basal aspect of CD ampullae and in the mesenchyme (Fig. 3b, e, h, k, n, q). Merge images reveal that only small areas of the SBA-positive micro-fibres show simultaneous labelling for Tgase2 (Fig. 3c, f, i, l, o, r). MMP-9 expression is detected in mesenchymal cells in close vicinity to both non-branching (Fig. 3b, e)

and branching (Fig. 3h, k) ampullae. In contrast, mesenchymal cells underneath the capsule fail to show MMP-9 expression. MMP-9 shows no preferred site of expression in the mesenchyme surrounding non-branched or branching CD ampullae. Thus, co-localisation of Tgase2 and MMP-9 occurs only in mesenchyme near by the cleft region between the dividing CD ampullae (Fig. 4).

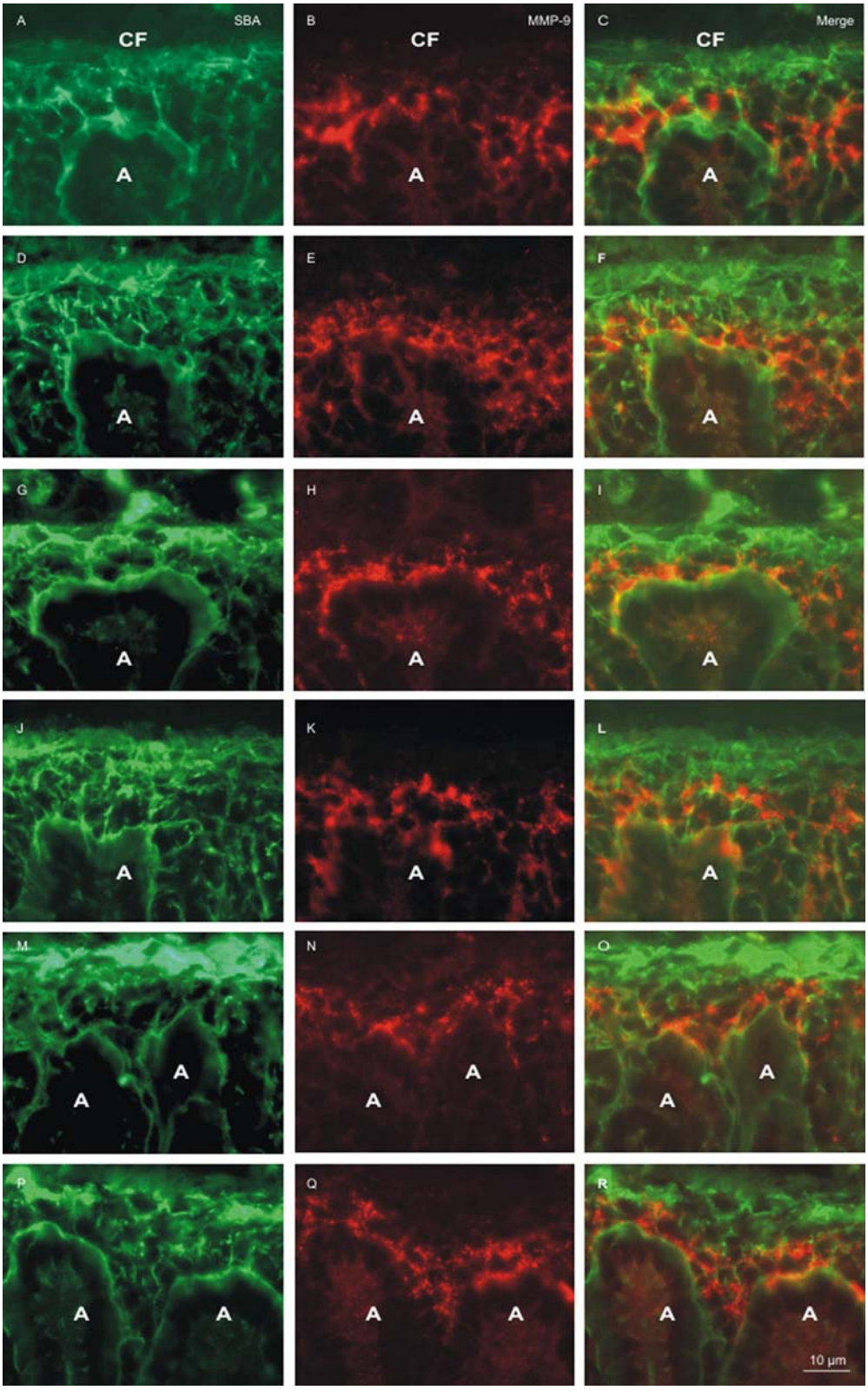

Fig. 3 Co-localisation of SBA-positive micro-fibres with the matrix-degrading enzyme MMP-9 at various developmental stages of CD ampulla branching (*A* CD ampulla, *CF* capsula fibrosa). *Left* SBA label (**a, d, g, j, m, p**). *Middle column* Label of MMP-9 (**b, e, h, k, n, q**). *Right* Merge image of the SBA label and the MMP-9 label (**c, f, i, l, o, r**). In non-branched CD ampulla (**a–f**), some fibres display partial co-localisation with the MMP-9-label. Similar results are obtained in CD ampulla revealing initiation of branching (**g–l**). Investigation of stages with deep cleft formation (**m–r**) shows that the MMP-9 expression occurs in the surrounding mesenchyme and at the basal aspect of the CD ampulla with no preferred location.

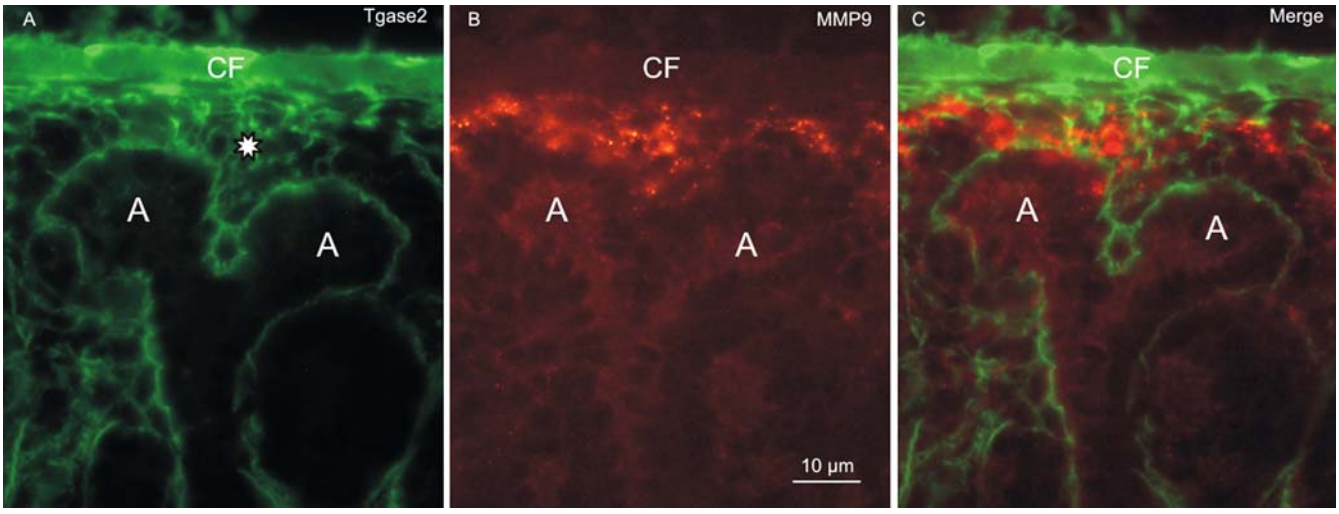

Fig. 4 Immunohistochemical co-localisation of Tgase2 (**a**) and MMP-9 (**b**) in branching CD ampullae (*A* CD ampulla, *CF* capsula fibrosa). **c** Co-localisation of both molecules in the central areas of the metanephric mesenchyme (*asterisk* in **a**) and at the basal aspect of CD ampulla (*A* CD ampulla, *CF* capsula fibrosa)

Source of Tgase2 and MMP-9

A further set of experiments was performed to analyse the tissue in which Tgase2 and MMP-9 was produced (Fig. 5). Mesenchymal cells and renal capsule were isolated from the embryonic zone of neonatal rabbit kidney by microsurgical methods under a binocular microscope. Isolated CD ampullae mechanically free of adherent mesenchymal cells and fragments of the organ capsule were impossible to find. Hence, data for CD ampulla are not shown. Analysis by RT-PCR demonstrated that pure mesenchymal cells or renal capsule expressed Tgase2 mRNA. Surprisingly, MMP-9 mRNA was found predominantly in the total extract of the embryonic zone, whereas mesenchyme and capsule showed little expression. These ressults indicated that the CD ampulla cells were the major source of MMP-9.

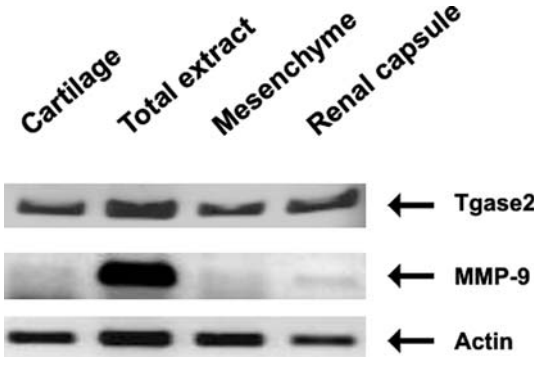

Fig. 5 mRNA expression of transglutaminase (Tgase2) and MMP-9 in the embryonic zone of neonatal rabbit kidney. Expression of Tgase2 is found in the extract of the embryonic zone, in the metanephric mesenchyme and in the renal capsule. Cartilage tissue, which is known to produce tissue Tgase2 mRNAs, served as a positive control. In contrast, strong MMP-9 mRNA label is found in the total extract of the embryonic area, whereas the mesenchyme and the renal capsule show only low MMP-9 mRNA expression.

Co-migration of SBA-postive proteins with Tgase2 and MMP-9 in SDS-PAGE

The presented histochemical data show that the SBA-labelled micro-fibres co-localise partially with Tgase2 and MMP-9 in the embryonic cortex of developing kidney. In addition, analysis of the amino acid sequence of Tgase2 and MMP-9 by post-translational modification prediction programms found at http://www.cbs.dtu.dk/services/NetOGlyc or http://www.cbs.dtu.dk/services/NetNGlyc indicates a potential glycosylation of both enzymes. Therefore, we analysed, in Western blotting experiments, whether Tgase2 and MMP-9 protein bands co-localised with bands found after SBA labelling. A band of 76 kDa was detected by the Tgase2 antibody and a band of 108 kDa was detected by the MMP-9 antibody. Both detected molecular weights were in accordance with the known molecular weights (http://www.cbs.dtu.dk). These results indicated the specificity of both antibodies. The obtained data show that the band for Tgase2 (76 kDa) and band for MMP-9 (108 kDa) co-migrate with SBA-labelled protein bands (Fig. 6). However, preincubation experiments with the antibodies against Tgase2 and MMP-9 before SBA probing did not alter the pattern of SBA-labelled protein bands and, vice-versa, neither did the addition of SBA before incubation with Tgase2 and MMP-9 antibodies (not shown), suggesting that the epitope bound by the Tgase2 or MMP-9 antibody differed from that of SBA-binding.

Co-migration of SBA-positive proteins with Tgase2 and MMP-9 in two-dimensional electrophoresis

Two-dimensional electrophoresis of the embryonic kidney cortex followed by Western blotting and SBA probing substantiated the experiments obtained after one-dimensional electrophoresis (Fig. 7). A comparison of the coordinates of the SBA-positive spots with the pI and molecular

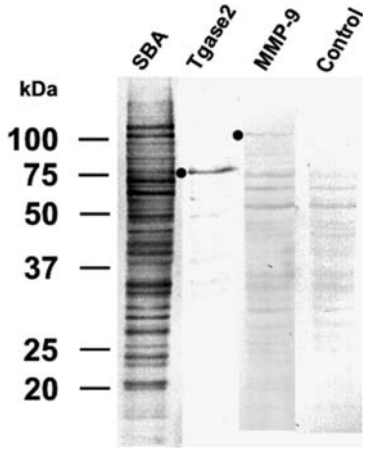

Fig. 6 SDS-PAGE of the embryonic cortex with subsequent Western blotting. Tgase2 probing reveals a 76-kDa band (*lower dot*). A specific band of 108 kDa was found for MMP-9 (*upper dot*). Both protein bands (108 and 76 kDa) co-migrate with bands obtained after SBA probing. The negative control was performed without the first antibody.

size of Tgase2 obtained by a database search (Swiss-Prot protein knowledgebase; http://us.expasy.org.prot/) revealed that one SBA-positive spot (pI 5.2; MW 76 kDa) corresponded to Tgase2. However, no two-dimensional protein labelling was obtained after MMP-9 antibody probing (not shown).

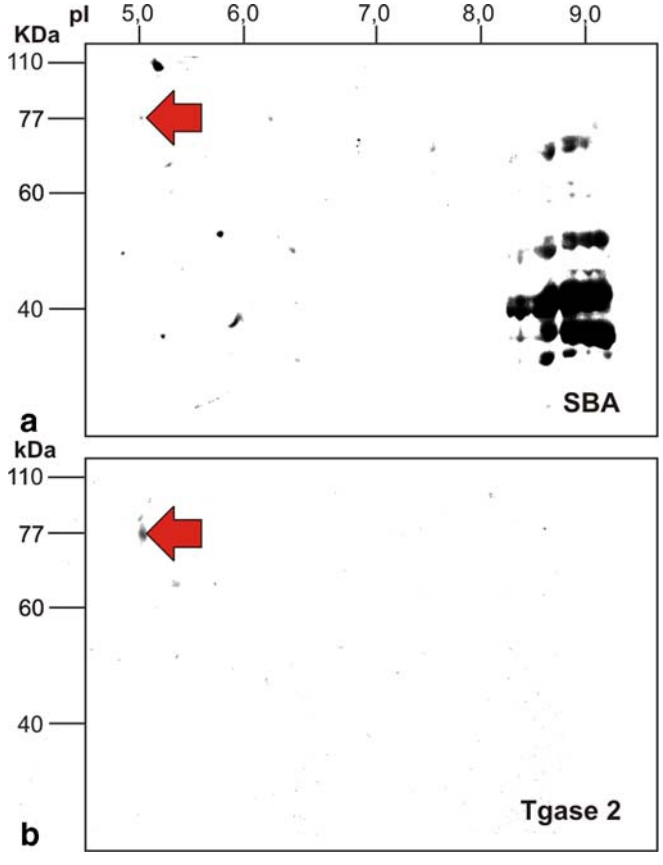

Fig. 7 Two-dimensional electrophoresis of the embryonic cortex with subsequent Western blotting. **a** Multiple spots are obtained after SBA probing. **b** One major spot is found after anti-Tgase2 antibody incubation, with the same pI (5.2) and the same molecular size (76 kDa) as the SBA-positive spot marked in **a** (*red arrows*)

Discussion

To date, it is unknown whether, in the developing kidney, the branching of the CD ampulla occurs randomly or whether guiding elements control the extension during organ growth. For continuous organ growth, the arising ampullae buds must remain in permanent contact with the overlaying competent mesenchyme. Otherwise, the induction of nephrons will fail (Smyth et al. 2003; Zhang et al. 2004).

Kidney histoarchitecture by growth cue or by accident

The area between each of the CD ampullae, the nephrogenic mesenchyme and the organ capsule shows unique features. Recent data indicate that, around the tip of each CD ampulla, a specific basement membrane is established that is entirely different from that of other tubuli (Strehl et al. 1997). As shown in the present study, the tissue can be labelled with SBA thus demonstrating that the micro-fibres originate from both non-branched and branching CD ampulla and line the cap condensate towards the capsule (Fig. 1). We have further demonstrated that SBA-positive micro-fibres are not microtubule- or actin-based structures. In contrast to data reported by Davies and co-workers (Fisher et al. 2001; Davies et al. 1995), we have found that the SBA-positive micro-fibres do not co-express laminin in the developing kidney of rabbit and mouse (Schumacher et al. 2003). Our results indicate that the micro-fibres are components of the ECM and that they differ from laminin-rich filaments (Schumacher et al. 2002a; Schumacher et al. 2003; Schumacher et al. 2002b). All these data suggest that the basal aspect of each CD ampulla, the related cap condensate and the organ capsule are structured by the SBA-positive micro-fibres during organ growth.

The volume growth of the kidney occurs in morphogenetic waves. It consists of a constantly repeating process including the temporal-spatial elongation and branching of the CD ampullae followed by the site-specific induction of nephrons. At a first glance, this appears to be a simple mechanism but it remains a non-understood process. In view of our data, we assume that the cells of the CD ampulla and the mesenchymal stem cells are fastened at the capsule by SBA-positive micro-fibres. When the organ grows, it increases in volume diameter. During this process, the close correlation between the CD ampulla, the surrrounding mesenchyme and the capsule needs to be preserved. A mechanical fastening by micro-fibres offers the advantage that the capsule will not lose contact with the mesenchyme and CD ampulla (Fig. 1c). This hypothesis is strengthened by the observation that it is impossible to isolate pure CD ampullae by microsurgical methods. Mesenchymal cells and capsule fragments constantly stick to the ampulla head.

Most probably, the described SBA-positive micro-fibres are responsible for this adherence. In addition, the distance of the CD ampulla to the organ capsule is constant. SBA-positive micro-fibres may be responsible for this structural invariant. It further may cause the precise longitudinal growth of the CD ampulla by continuous passive stretching towards the capsule.

Not only the elongation of the CD ampullae, but also their arborisation is controlled during organ growth. First of all, the geometrical branching direction is determined by an unknown mechanism. Thus, increased mitosis in the future bud part of the CD ampulla cells has to be up-regulated so that the bifurcation will be clearly oriented. For example, it would severely disturb the development of the renal structure if one bud grew towards the capsule, while another grew towards the medulla. In normal kidney development, both buds are oriented in a remarkable order towards the capsule. The constant distance of the buds to the capsule in conjunction with the SBA-positive micro-fibres makes it probable that the dichotomous branching of the CD ampulla does not occur by chance but by a growth cue, most probably in the form of the SBA-positive micro-fibres.

Modulation of the ECM during organ expansion

The degradation and modulation of ECM molecules are essential processes for nephrogenesis and CD ampulla growth. Tgase2 is able to cross-link proteins through an acyl-transfer reaction between the g-carboxamide group of peptide-bound glutamine and the e-amino group of peptide-bound lysine (Ohtsuka et al. 2000). The result of this reaction is a e-(g-glutamyl) lysine isopeptide bond. In the extracellular space, the enzyme is able to cross-link molecules such as fibronectin (Martinez et al. 1989). This biological function enables the stabilisation of various proteins. Tgase2 is also known to facilitate cell adhesion (Verderio et al. 2003) and cell motility (Mohan et al. 2003). It may also utilises fibronectin as an alternate substrate. In this context, fibronectin has been noted as being an essential molecule for branching morphogenesis (Sakai et al. 2003). It is transiently expressed in the cleft region of salivary gland buds. Since fibronectin is the major substrate of tissue Tgase2 in other tissues, it would be interesting to investigate whether bud formation can be influenced by Tgase2.

MMP-9s and their inhibitors (TIMPs) play an important role in kidney development (Legallicier et al. 2001). The detection of Tgase2 in addition to the known occurrence of MMP-9 in our study shows that not only matrix-degrading but also matrix-stabilising enzymes are involved in nephrogenesis. We demonstrate that the SBA-positive micro-fibres in part co-localise with Tgase2 (Fig. 2) and MMP-9 (Fig. 3). Thus, both enzymes probably use the SBA-positive micro-fibres as a substrate.

For the first time, Tgase2 has been demonstrated as an enzyme for ECM stabilisation found at the basal aspect of the CD ampulla, within the cap condensate and in the capsule (Fig. 2). The most intensive label is detected on non-branched (Fig. 2b, e) ampullae and on ampullae embarking on branching out (Fig. 2h, k), whereas further branched (Fig. 2n, q) ampullae show a signal restricted to the cleft between the arising buds. Consequently, the presence of the label depends on the arborisation of the CD ampulla.

The temporal-spatial process of CD ampulla branching is inversely correlated with MMP-9 occurence (Fig. 3). Areas have been found in which MMP-9 is detected only within a thin layer of mesenchymal cells in the vicinity of the CD ampullae, whereas the mesenchyme beyond the capsule is not labelled (Fig. 3b, e, h, k, n, q). In contrast, other areas exist in which moderate MMP-9 label is seen in the mesenchyme between branching ampullae (Fig. 3n, q). Thus, the immunolabel for MMP-9 reveals a striking microheterogeneity within the mesenchyme of embryonic renal tissue. This microheterogeneity is obviously related to the temporal-spatial branching process of the CD ampullae.

In summary, our data reveal the temporal-spatial co-localisation of Tgase2 and MMP-9 with SBA-positive micro-fibres in the mammalian embryonic kidney cortex. Our results suggest that the microfibres are modulated during the growth and arborisation of the CD ampulla by both enzymes. We assume that the micro-fibres that co-localise with Tgase2 are stabilzed by the enzyme so that degradation of the micro-fibres by MMP-9 is prevented. The interplay of both enzymes with the SBA-positive micro-fibres could be the mechanism that controls the direction of the growth of the CD ampulla. This aspect has to be further investigated by using Tgase2 and MMP-9 knockout mice.

The molecules that regulate the interaction between Tgase2 and MMP-9 in embryonic renal tissue remain to be investigated. Retinoid acid and TGFβ are known to be able to modulate Tgase2 expression in adult tissue (Douthwaite et al. 1999; Singh et al. 2001) and to influence CD ampulla growth (Ritvos et al. 1995). Thus, future culture experiments may clarify whether both molecules can modulate the expression of Tgase2 and MMP-9 in embryonic tissue and, in turn, whether this effect influences the occurrence of the SBA-positive fibres.

Acknowledgements The technical help of Mrs. L. Denk and Mrs. S. Lukas is gratefully acknowledged. We thank Dr. Hayo Castrop for critical comments.

References

Barasch J, Yang J, Ware CB, Taga T, Yoshida K, Erdjument-Bromage H, Tempst P, Parravicini E, Malach S, Aranoff T, Oliver JA (1999) Mesenchymal to epithelial conversion in rat metanephros is induced by LIF. Cell 99:377–386

Bard JB, Gordon A, Sharp L, Sellers WI (2001) Early nephron formation in the developing mouse kidney. J Anat 199:385–392

Davies J, Lyon M, Gallagher J, Garrod D (1995) Sulphated proteoglycan is required for collecting duct growth and branching but not nephron formation during kidney development. Development 121:1507–1517

Dekel B, Reisner Y (2004) Embryonic committed stem cells as a solution to kidney donor shortage. Expert Opin Biol Ther 4:443–454

Douthwaite JA, Johnson TS, Haylor JL, Watson P, El Nahas AM (1999) Effects of transforming growth factor-beta1 on renal extracellular matrix components and their regulating proteins. J Am Soc Nephrol 10:2109–2119

Fisher CE, Michael L, Barnett MW, Davies JA, Davies J, Lyon M, Gallagher J, Garrod D (2001) Erk MAP kinase regulates branching morphogenesis in the developing mouse kidney: sulphated proteoglycan is required for collecting duct growth and branching but not nephron formation during kidney development. Development 128:4329–4338

Kim SY, Jeong EJ, Steinert PM (2002) IFN-gamma induces transglutaminase 2 expression in rat small intestinal cells. J Interferon Cytokine Res 22:677–682

Legallicier B, Trugnan G, Murphy G, Lelongt B, Ronco P (2001) Expression of the type IV collagenase system during mouse kidney development and tubule segmentation. J Am Soc Nephrol 12:2358–2369

Martinez J, Rich E, Barsigian C (1989) Transglutaminase-mediated cross-linking of fibrinogen by human umbilical vein endothelial cells. J Biol Chem 264:20502–20508

Minuth WW (1987) Neonatal rabbit kidney cortex in culture as tool for the study of collecting duct formation and nephron differentiation. Differentiation 36:12–22

Mohan K, Pinto D, Issekutz TB (2003) Identification of tissue transglutaminase as a novel molecule involved in human CD8+ T cell transendothelial migration. J Immunol 171:3179–3186

Ohtsuka T, Ota M, Nio N, Motoki M (2000) Comparison of substrate specifities of transglutaminase using synthetic peptides as acyl donors. Biosci Biotechnol Biochem 64:2608–2613

Plisov SY, Yoshino K, Dove LF, Higinbotham KG, Rubin JS, Perantoni AO (2001) TGF beta 2, LIF and FGF2 cooperate to induce nephrogenesis. Development 128:1045–1057

Ritvos O, Tuuri T, Eramaa M, Sainio K, Hilden K, Saxen L, Gilbert SF (1995) Activin disrupts epithelial branching morphogenesis in developing glandular organs of the mouse. Mech Dev 50:229–245

Sakai T, Larsen M, Yamada KM (2003) Fibronectin requirement in branching morphogenesis. Nature 423:876–881

Sariola H (2002) Nephron induction revisited: from caps to condensates. Curr Opin Nephrol Hypertens 11:17–21

Saxen L (1987) Organogenesis of the kidney. Cambridge University Press, Cambridge

Schumacher K, Strehl R, De Vries U, Groene HJ, Minuth WW (2002a) SBA-positive fibers between the CD ampulla, mesenchyme, and renal capsule. J Am Soc Nephrol 13:2446–2453

Schumacher K, Strehl R, Minuth WW (2002b) Detection of glycosylated sites in embryonic rabbit kidney by lectin chemistry. Histochem Cell Biol 118:79–87

Schumacher K, Strehl R, Minuth WW (2003) Characterization of micro-fibers at the interface between the renal collecting duct ampulla and the cap condensate. Nephron Exp Nephrol 95:e43–e54

Singh US, Kunar MT, Kao YL, Baker KM (2001) Role of transglutaminase II in retinoic acid-induced activation of RhoA-associated kinase-2. Embo J 20:2413–2423

Smyth BJ, Snyder RW, Balkovetz DF, Lipschutz JH (2003) Recent advances in the cell biology of polycystic kidney disease. Int Rev Cytol 231:51–89

Strehl R, Minuth WW (2001a) Partial identification of the mab (CD) Amp1 antigen at the epithelial-mesenchymal interface in the developing kidney. Histochem Cell Biol 116:389–396

Strehl R, Minuth WW (2001b) Nephron induction–the epithelial mesenchymal interface revisited. Pediatr Nephrol 16:38–40

Strehl R, Kloth S, Aigner J, Steiner P, Minuth WW (1997) PCDAmp1, a new antigen at the interface of the embryonic collecting duct epithelium and the nephrogenic mesenchyme. Kidney Int 52:1469–1477

Tanney DC, Feng L, Pollock AS, Lovett DH (1998) Regulated expression of matrix metalloproteinases and TIMP in nephrogenesis. Dev Dyn 213:121–129

Tezuka K, Nemoto K, Tezuka Y, Sato T, Ikeda Y, Kobori M, Kawashima H, Eguchi H, Hakeda Y, Kumegawa M (1994) Identification of matrix metalloproteinase 9 in rabbit osteoclasts. J Biol Chem 269:15006–15009

Vainio S, Lehtonen E, Jalkanen M, Bernfield M, Saxen L (1989) Epithelial-mesenchymal interactions regulate the stage-specific expression of a cell surface proteoglycan, syndecan, in the developing kidney. Dev Biol 134:382–391

Verderio EA, Telci D, Okoye A, Melino G, Griffin M (2003) A novel RGD-independent cell adhesion pathway mediated by fibronectin-bound tissue transglutaminase rescues cells from anoikis. J Biol Chem 278:42604–42614

Zhang MZ, Mai W, Li C, Cho SY, Hao C, Moeckel G, Zhao R, Kim I, Wang J, Xiong H, Wang H, Sato Y, Wu Y, Nakanuma Y, Lilova M, Pei Y, Harris RC, Li S, Coffey RJ, Sun L, Wu D, Chen XZ, Breyer MD, Zhao ZJ, McKanna JA, Wu G (2004) PKHD1 protein encoded by the gene for autosomal recessive polycystic kidney disease associates with basal bodies and primary cilia in renal epithelial cells. Proc Natl Acad Sci USA 101:2311–2316